Proceedings of the 1996 IEEE
International Conference on Robotics and Automation
Minneapolis, Minnesota - April 1996

Development of a Dynamic Biped Walking System for Humanoid
- Development of a Biped Walking Robot Adapting to the Humans' Living Floor -

Jin'ichi Yamaguchi**, Noboru Kinoshita*, Atsuo Takanishi**, and Ichiro Kato**

* **Department of Mechanical Engineering School of Science and Engineering, and
**Humanoid Research Laboratory, Advanced Research Center for Science and Engineering,
Waseda University,
3-4-1, Okubo, Shinjyuku-ku, Tokyo, 169, Japan

Abstract

In this paper, the authors introduce an anthropomorphic dynamic biped walking robot adapting to the humans' living floor. The robot has two remarkable systems: (1) a special foot system to obtain the position relative to a landing surface and the gradient of the surface during its dynamic walking; (2) an adaptive walking control system to adapt to the path surfaces with unknown shapes by utilizing the information of landing surface, obtained by the foot system. Two units of the foot system WAF-3 were produced, a biped walking robot WL-12RVII that had the foot system and the adaptive walking control system installed inside it was developed, and a walking experiment with WL-12RVII was performed. As a result, dynamic biped walking adapting to humans' living floor with unknown shape was realized. The maximum walking speed was 1.28 s/step with a 0.3 m step length, and the adaptable deviation range was from -16 to +16 mm/step in the vertical direction, and from -3 to +3 ° in the tilt angle.

1 Introduction

The control systems of conventional anthropomorphic dynamic walking robots studied in the past required that the information on the accurate shapes of the paths on which the robots walked were available before implementation of dynamic walking or that of the swing leg landing control [1]-[7],[9]. However, neither the accuracy of the lower-limbs trajectory nor that of the measurement of the path surface shape demanded to maintain 3-dimensional stable dynamic walking have been referred to by any reports [1]-[8].

Although WL-12RV (Waseda Leg-12 Refined V) showed the most stable dynamic biped walking among the biped walking robots which were developed by Waseda University earlier than 1991[9], it became clear that the robot received influences of the lower-limbs trajectory deviation and the walking surface shape deviation more and more as the walking speed increased. In the pace of one step per second just like a human, the robot must satisfy the accuracy of a few millimeters in terms of the height of path surfaces and that of approximately 0.5 degree for the gradient of path surfaces, otherwise, since an adverse influence to dynamic walking caused by the foot landing position deviation occurring at the landing of the swing leg may not attenuate within the one stride so that it becomes unable to ensure the maintenance of 3-dimensional stable dynamic walking.

In contrast, in the actual environment where humans live, it is very rare that path surfaces have the characteristics of a geometric plane, with deformation by some ruggedness and undulation in almost all cases. The result shows that the robot cannot make stable dynamic walking in the environment. Study on the Humanoid is being done as the Project: Humanoid at HUREL (HUmanoid REsearch Laboratory), Advanced Research Center for Science and Engineering, Waseda University. Therefore, the authors feel that it is time to develop a dynamic biped walking adapting to the real world.

It is considered mainly because the conventional control method of dynamic biped walking constituted an open loop control system that only indirectly controls the leg trajectory relative to the landing surface relying on internal sensors in spite of a fact that walking is a series of movements made against the landing surface.

In 1985, Takanishi tried to detect the shapes of path surfaces by the robot itself using WL-10RD (Waseda Leg-10 Refined Dynamic)[5]. The robot employed a torque control on the ankle joints but, since they could not absorb sufficiently the impact occurring at landing of swing leg and the robot itself vibrated during dynamic walking so that it was impossible to obtain the information of landing surfaces throughout all phases of dynamic walking.

On the other hand, the human body is considered to have functions that utilize the pliable tissues which cover hard bones, to absorb impacts of collision even in movements accompanying collisions against external environment so as to prevent vibrations occurring both on himself and the object of collision and obtain various information concerning the latter. Many human movements accompany collisions with external environment and these functions are considered to facilitate very much the construction of closed loop control using external sensors.

From foregoing considerations, the purpose of this study was to develop a foot mechanism which mounts a landing surface detection system, as an external sensor, which measures the gradient of the landing surface during dynamic walking as well as the relative position to the surface, to devise a walking control method that constitutes a closed loop control system which provides a lower-limbs trajectory control against the landing surface on the real time basis by utilizing the information of the landing surface, obtained by the above mentioned foot mechanism, and to develop a life size biped walking robot which adapt to the actual world in which the lower-limbs trajectory deviation and the surface shape deviation can not be

0-7803-2988-4/96 $4.00 © 1996 IEEE

reduced to zero.

2 Required condition of the walking surface

Required condition of the walking surface to be researched was set as follows.

(1) Height and gradient of the path surface are unknown factors.

(2) All landing spikes (see **Fig. 4**) in the four corners of the biped walking robot's foot must be able to be grounded.

(3) Extent of deform of the path surface and that of movement that are experienced when the machine model walks, are limited to the ranges that there is no need to make the compensating movement that considers the dynamics.

It should be noted that the gradient of lateral plane is provided to be horizontal (Accuracy $\pm 0.5^{\circ}$) and known in advance. This is because the present WL-12 Series has no active degree of freedom around the roll axis of the lower-limbs, regarding materials of the surface, such that does not deform at all when the machine model walks and that sags approximately 2 mm when it is standing on single leg, satisfy the conditions.

Take for instance the flooring materials which are generally used in the human living environment, it is learned that the floor which is not likely to deform, such floor covered with a carpet and other flooring materials which may deform slightly such as the tatami mattress and the like, satisfy such conditions.

3. Biped walking robot WL-12RVII

3.1 Machine model

This machine model is an improved version of a biped walking robot WL-12RVI [10], which is equipped with a trunk mechanism to compensate for three-axis moment by trunk motion and the foot mechanism WAF-2 (Waseda Anthropomorphic Foot No. 2)**[11]** to acquire a relative position to the landing surface. The new version incorporated modifications that were required by the mounting of the newly developed foot unit WAF-3 (Waseda Anthropomorphic Foot No. 3) and was named Waseda Leg No. 12 Refined VII (WL-12RVII). The total weight of the robot is 109 Kg, the weight of the trunk is 30.0 Kg, and the height in a static straight standing trunk position is 1866 millimeters. An assembly drawing of this machine is illustrated in **Fig. 1**. The link structure and assignment of active DOFs (degrees of freedom) are illustrated in **Fig. 2**. The total active DOF of this machine is 9 DOF, which is the same as that of WL-12RVI, consisting of 6 DOF for the pitch axes of the lower limbs, and 1 DOF for each of the pitch axis, roll axis, and yaw axis of the trunk (3 DOF for the trunk). The actuators each employ an electric hydraulic servo system combining a hydraulic RA (rotary actuator) and a servo valve. The maximum torque of the actuator is 300 Nm and the maximum angular velocity about 150 degree per sec.

Furthermore, this machine has the capability of autonomously executing real-time controls, which require high-speed processing, with no external assistance because it is equipped with four units of 16 bit CPUs for controlling individual actuators and two units of 32 bit RISC processors for generating walking patterns on a real-time basis. The configuration of the computer system mounted on this robot is illustrated in **Fig. 3**. A local position feedback system of a high gain ratio was applied to each joint of the robot during walking.

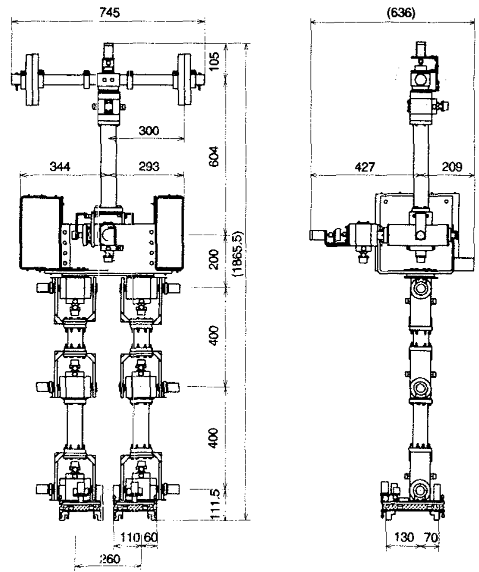

Fig. 1 Assembly drawing of WL-12RVII

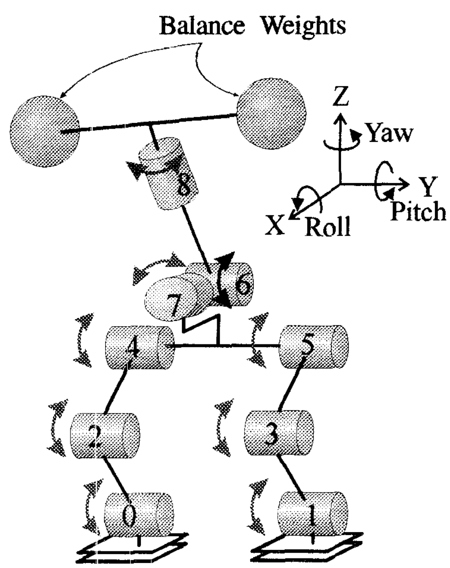

Fig. 2 Link structure of WL-12RVII

3.2 Foot Mechanism WAF-3

Like a man's palm, finger pad and sole, although WAF-3 is flexible, it does not transform any further when load is applied up to a point because of its nonlinear hardness property. WAF-3 is also equipped with sensors enough to detect the shapes and the gradient of the path surfaces during dynamic biped walking.

Fig. 4 presents a rough sketch of WAF-3 and the detection coordinate O'-X'Y'Z' which was established up in order to measure the landing path surface. This mechanism consists of an upper foot plate which is directly fitted to the foot beneath the ankle actuator, a lower foot plate which directly makes contact with the path surface, several pieces of wire which connect the upper foot plate and the lower foot plate, and a sandwich structure which clamps an open-cell-foam shock absorbing material between the upper foot plate and the lower foot plate.

In reference to the movable range (MR) of the passive DOF of human lower-limbs, a similar range was set for WAF-3. Specifically, on Cartesian coordinates as shown in **Fig. 4**, the MR on X' axis was set at ± 5.0 mm, the MR on Z' axis was set at 5.5 mm, the MR around X' axis was set at ± 2.3 °, and the MR around Y' axis was set at ± 1.7 °. The weight of this foot unit is 3.0 kg for one leg, i.e., 1.8 Kg heavier than the conventional foot weight of the WL-12RV. The mechanisms which WAF-3 possesses are summarized below.

(A) Shock absorbing mechanism

(B) Support leg change stabilization mechanism

(C) Landing path surface detection mechanism

The following describes the individual mechanisms.

(A) Shock absorbing mechanism: WAF-3 has a passive shock absorbing mechanism which uses shock absorbing material to enable "high-speed following operation to the landing surface, the buffer of the impact which occurs when the swing foot touches the ground, control of the vibration caused in the robot during dynamic biped walking", which are difficult to be handled by the feedback control with software which uses information obtained by the force sensor installed below the foot plate [8].

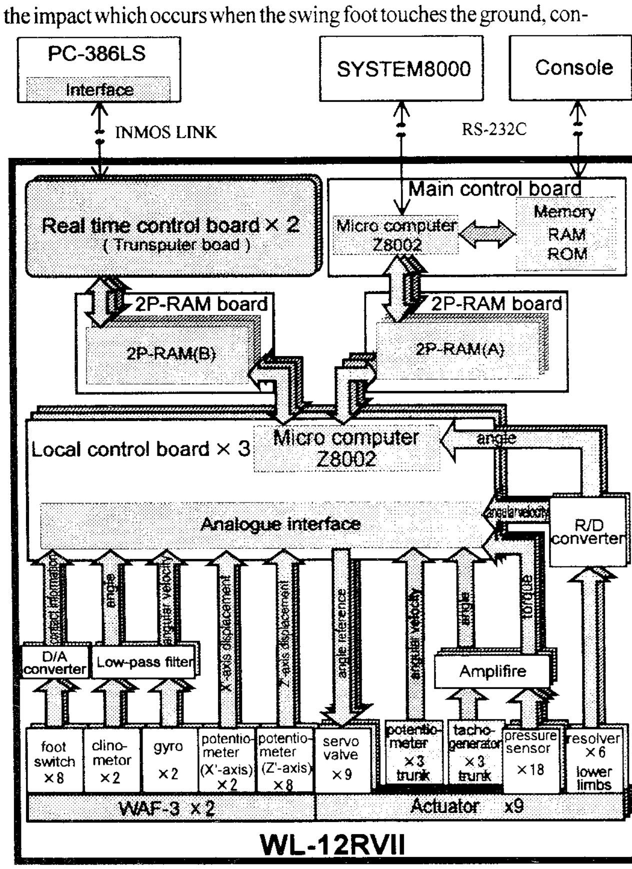

Fig. 3 Computer System structure of WL-12RVII

The shock absorbing mechanism consists of two main parts: **(A-a)** shock absorbing material installed between the two foot plates; **(A-b)** silicon foam and two layers of polyurethane rubber sheeting on Teflon resin arranged in parallel beneath the upper stoppers. Such structures provided a shock absorbing mechanism that has a human nonlinear characteristic with the smooth rise of stiffness against force.

With respect to **(A-a)** the shock absorbing material, "Memory foam M-36 yellow (216 cm^2, 25 mm thick)" (E.A.R. SPECIALTY COMPOSITES Corporation, product name in the U. S., Confor Foam), marketed by YAMAMITSU OIL Ltd. in Japan was selected because it has excellent characteristics in terms of shock absorption, durability, and flexibility, and it has an open-cell structure. This material was fitted to the foot in the state compressed to a thickness of 20 mm without any load applied to the foot. With approximately over 120 Nm, the material is compressed to a thickness of 14.5 mm. On that occasion, the alteration of stiffness characteristics with temperature is prevented by keeping a temperature of foot mechanisms at nearly 40°C by the heater, because the stiffness characteristic of the shock absorbing material used against impacts may be altered according to the specific temperatures. In the case that the material was fitted to the foot mechanism, the damping coefficient was approximately 40.6 Kg•s/m in the direction of shrinkage.

(B) Stabilization mechanism of support leg change: WAF-3 has the same stabilization mechanism of support leg change as WAF-2. Combining this mechanism with shock absorbing mechanism gives a biped walking robot robustness to total deviation of about one degree in the tilt angle, about several millimeters in the direction of Z' axis, and about 5 mm in the direction of X' axis-total deviation including the deviations of the measured path-surface shape and the lower-limbs trajectory. Refer to **document [11]** for details of this mechanism.

(C) Detection mechanism of landing path surface: In order to accomplish an adaptive walking on humans' living path surface, This mechanism is capable of obtaining the following information about the landing surface.

(C-a) The information on the grounding of the lower-foot plate

(C-b) The relative position to the landing surface (lower-foot plate)

(C-c) The gradient of the landing surface (around Y' axis)

(C-d) The angular velocity of the upper-foot plate (around Y' axis)

Explanatory to say about each installed sensor, **(C-a)** WAF-3 has microswitches with levers in the four corners of the lower surface of the lower-foot plate, to detect the grounding of the lower-foot plate. These microswitches have a lever with convex shape in its central part, and they have an attaching position within the support polygon formed with the landing spikes and the landing surface, to prevent the damage during dynamic walking. **(C-b)** A linear potentiometer with back spring is installed at each of the four corners of the upper-foot plate. The four linear potentiometers are intended to indirectly measure the relative position to the path surface through measurement of the top plane of the lower foot plate that performs landing following the shape of path surface. **(C-c)** It has a servo-type inclination sensor on the upper side

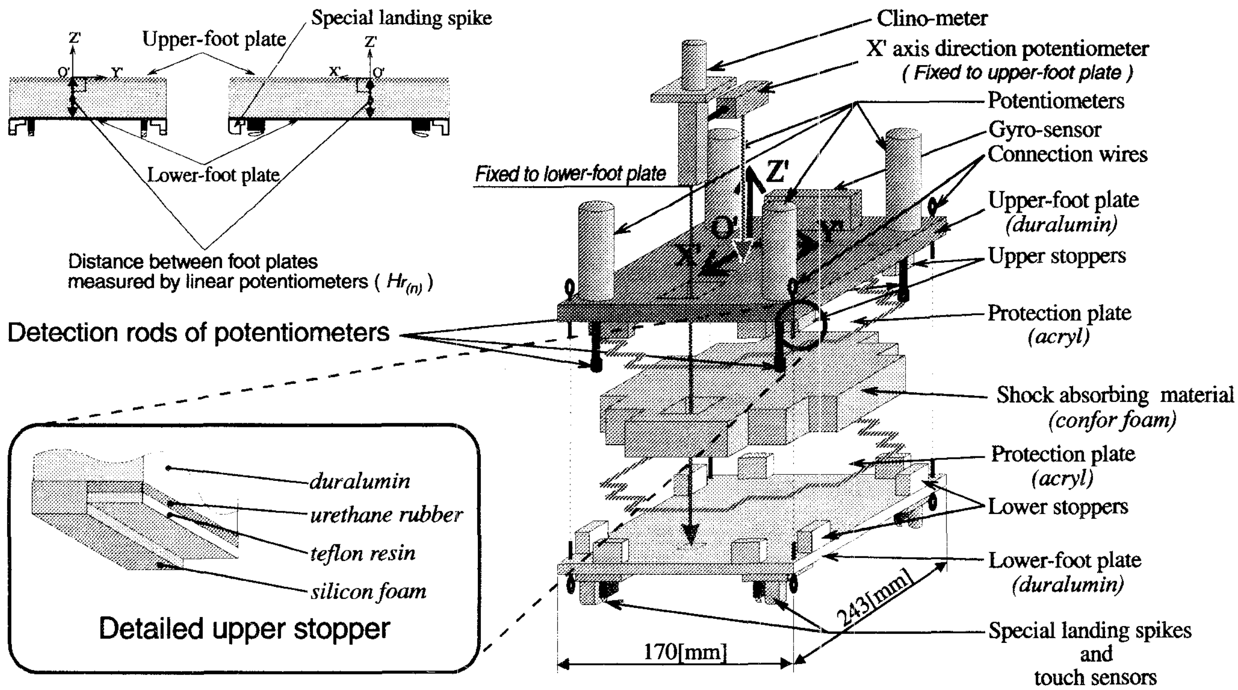

Fig. 4 Structure of WAF-3, O'-X'Y'Z': detection coordinate.

of the lower-foot plate through the duralumin block for attaching a sensor and the like, to measure a gradient of the landing surface (around Y' axis). **(C-d)** It has a vibrating gyro on the upper-foot plate, to measure an angular velocity of the upper-foot plate and to presume a gradient of the upper-foot plate (around Y' axis). The sampling frequency of the output of the sensors is set to 100 Hz. On that occasion, concerning a gradient of the path surface, the horizontal was set as an origin, and it was defined that the direction being uphill with the robot's advance in the positive.

4 Walking control method

The biped walking control method on which we report in this paper uses a three-layer structure as shown in **Fig. 5** for the stabilization of dynamic biped walking to obtain high stability as the locomotion mechanism of a humanoid.

Basic stabilization control of biped walking uses the biped walking control method that we have already proposed in **document [9]**.

Next, stabilization devices located above the method are shock absorbing mechanism and support leg change stabilization mechanism. These mechanisms remove the influences on walking by "measurement errors of the path-surface shape and the lower-limbs trajectory deviation caused by the bend of the structural members of the machine model, etc.", which is not considered in the above-mentioned walking control method. These double stabilizing systems allow the robot to continue dynamic biped walking, even if we program-control the robot considering slightly transformable path surface like the horizontal wooden floor covered with a carpet as horizontal and smooth, when the lower-limbs trajectory deviation of the robot is within several millimeters.

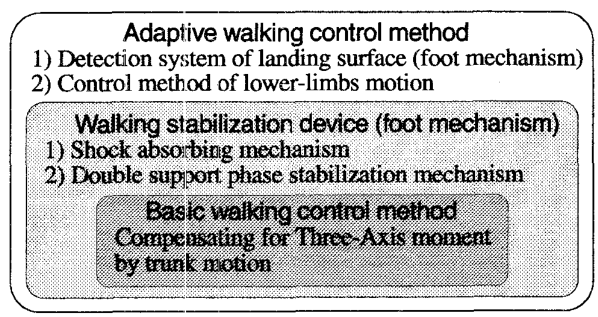

Fig. 5 Stabilization of dynamic biped walking in the real world

Finally, the stabilization control located the highest is adaptive walking control system, which is proposed in this paper. This control system is closed loop control system that acquires position information of the robot in the external world from the landing path surface detection mechanism and changes the lower-limbs trajectory based on the information. The purpose of the system is for humanoid to continue stable dynamic walking even if It meets the amount of path-surface shape deviation and the lower-limbs trajectory deviation its walking stabilization device can not cope with. Moreover, we think that the ability to continue stable dynamic biped walking in spite of some deviation in the shape of the path surface is important because it will reduce the load of the visual system of a humanoid.

The following is an outline of the adaptive walking control system: First, a robot walks using a walking pattern (hereafter, the authors refer to this pattern as the standard walking pattern) for a flat floor. Second, the robot obtains information about landing surface using WAF-3. Using this information, the robot at the same time changes and controls the lower-limbs motion to adapt to the unknown landing surface on a real time basis. Besides, the robot's walking is suitable to the path surface with deviation in the inclination in addition to the height, without worrying about the emanation of lower-limbs motion, by combining the control for returning to the standard walking pattern every one step. By repeating this, the walk suitable to path surfaces with deviation is done in real time through all walking periods, also concerning the inclination of path surfaces in addition to the height of path surfaces. On that occasion, in the creation of the standard walking pattern, the control method of trunk-compensated, bipedal-locomotive is used, being proposed by the authors. As for lower-limb trajectories used for that, the trajectory of the lower side of foot parts is set with constant leveling. A flow chart of this walking control method is shown in **Fig. 6**.

A processing method of the information on the landing surface acquired and the control methods of lower-limb trajectories, which are vital factors in the system, are described below.

4.1 Processing method of information on landing surfaces

All kinds of information acquired by this mechanism for detecting a landing surface is sent to the computer for controlling in real time in walking, and arranged into the following information. **Fig. 7** shows each system of coordinates set to the walking system.

(1) The information on the grounding of the lower-foot plate: The grounding is judged with ON/OFF of the microswitches installed in the four corners of the lower side of the lower-foot plate. Basically, the leg was judged grounding when all microswitches in the four corners turn on.

(2) The information on the relative angle and the relative distance of landing surfaces and upper-foot plates: With respect to obtaining the relative position to the landing surface, it is possible to determine a plane based on the measurement of the positions of three

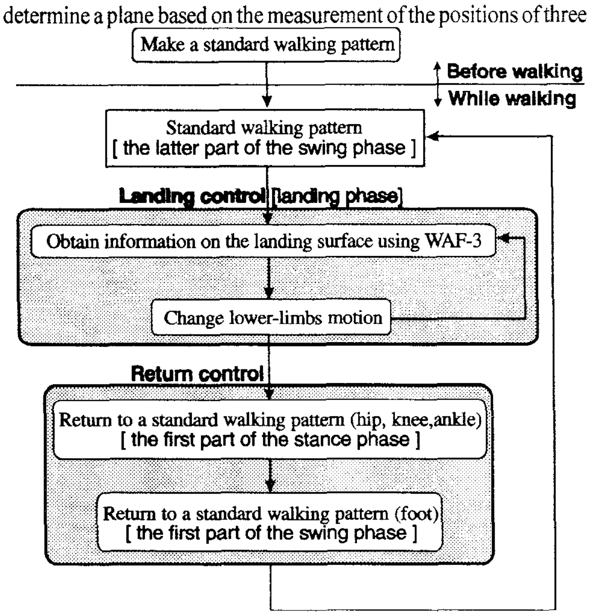

Fig. 6 Outline of the adaptive walking control method

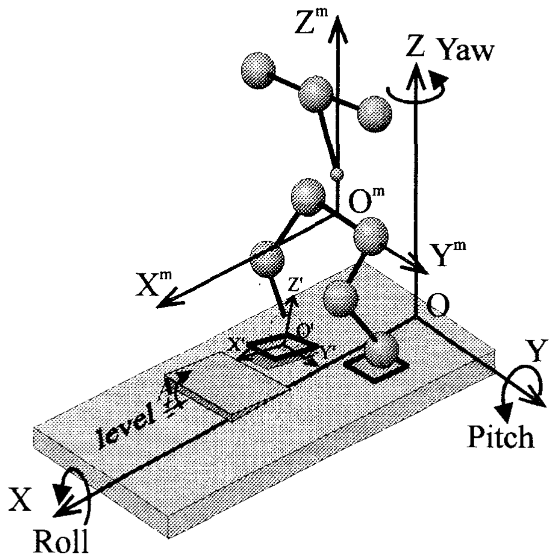

O^m-$X^mY^mZ^m$: moving coordinate
O-XYZ : fixed coordinate
O'-X'Y'Z' : detection coordinate

Fig. 7 Coordinate systems for adaptive walking

points. However, linear potentiometers were determined to be fitted to the four corners of the upper surface of the upper-foot plate in order to make it easy to evaluate the information about contact with path surfaces and to improve the accuracy of path surface detection by averaging the measurements of three points in two ways. The four linear potentiometers are intended to indirectly measure the relative angle A' (*around* Y' axis) and the relative distance Hr to the path surface through measurement of the top plane of the lower- foot plate that performs landing following the shape of path surface.

(3) The gradient of landing surfaces: The gradient of landing surfaces is calculated (presumed and measured), by using the value output by the rate gyro fixed on the upper side of the upper-foot plate to be integrated and the value output by the clinometer fixed on the lower-foot plate through the attaching block and the like. On that occasion, the gradient of landing surfaces is calculated by using the expression **(1)**.

$$A_n = \begin{cases} (Ac_n + A_{n-1} + A_{n-2})/3 \ldots\ldots\text{(stance phase)} \\ (Ag_n + A_{n-1})/2 \ldots\ldots\ldots\ldots\text{(landing phase)} \\ Ag_n \ldots\ldots\ldots\ldots\ldots\ldots\text{(swing phase)} \end{cases} \quad \mathbf{(1)}$$

A_n: The estimated value of the gradient of landing surfaces, in the detection of landing surfaces at "n" times.

Ac_n: The gradient acquired by clinometers, in the detection of landing surfaces at "n" times.

Ag_n: The result of which the relative angle of the upper- and the lower-foot plates (A' is added to the inclination value obtained from the value integrated by rate-gyro sensors (100 Hz), in the detection of landing surfaces at "n" times.

The detection frequency is set 32 per one step. The outline of the

Table 1 Division control of lower-limbs motion

	one stride							
Right leg	stance phase (double support phase)	swing phase		landing phase	stance phase (double support phase)	stance phase (single support phase)		
	(Ⅲ-c)	(Ⅳ)	(Ⅰ)	(Ⅱ)	(Ⅲ-a)	(Ⅲ-b)	(Ⅲ-c)	
Left leg	stance phase (double support phase)	stance phase (single support phase)			stance phase (double support phase)	swing phase		landing phase
	(Ⅲ-a)	(Ⅲ-b)	(Ⅲ-c)		(Ⅲ-c)	(Ⅳ)	(Ⅰ)	(Ⅱ)

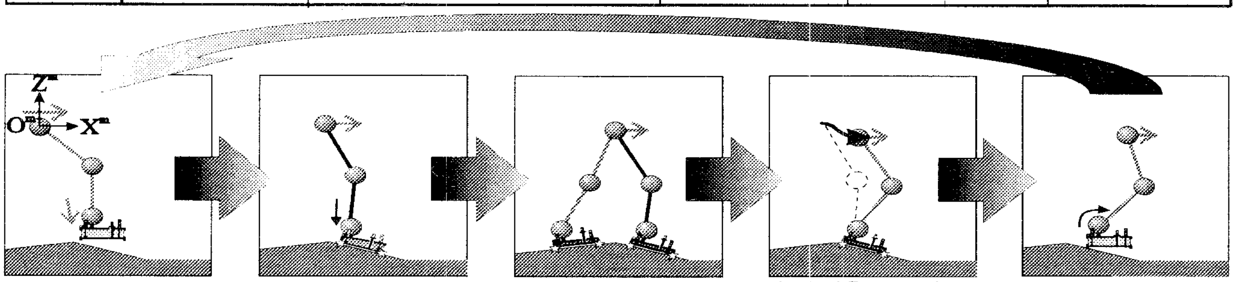

(Ⅰ) Standard motion [swing phase (latter)] (Ⅱ) Landing motion [landing phase] (Ⅲ-a) Modified motion [double-support phase] (Ⅲ-b, c) Return motion (hip,knee,ankle) [single-support phase (former)] (Ⅳ) Return motion (foot) [swing phase (former)]

Fig. 8 Walking actions adapting to the ground geometry in one step-walking

method for calculating a gradient of landing surfaces (around Y' axis) by the expression **(1)** is as follows. First of all, at the swing and the landing phases, the gradient of landing surfaces is presumed, by adding the relative angle (around Y' axis) acquired by the direct-acting potentiometer with the landing surface to the angle information time-integrated the value output by the rate-gyro sensor (the angular velocity). Next, at the double and the single support phases after finishing the vibration caused by landing, the information time-integrated the value output by rate-gyro sensor is corrected, while the gradient of the landing surfaces is measured by the value output by the clinometer. Like these, the authors thought that the gradient of the landing surfaces will be measured in dynamic walking with a short double-support phase, by using the two sensors complementary. The shock absorbing mechanism is essential in measuring the gradient of the landing surface during dynamic walking. Because this mechanism suppresses the vibration generated by landing shock and the robot itself, we can perform high precision measurement (Accuracy $\pm 0.5^\circ$) of the gradient of the landing surface (see **Fig. 10**).

4.2 Method of Lower-limbs Motion Modification

In this control method of walking, the one-step phase is largely divided into the three phases such as the swing phase with no restriction, the support phase with full restriction, and the landing phase of intermediate, and the swing phase and the support phase are divided into the double support phase and the former and the latter single support phase additionally, according to the degree of which the feet of robots are restricted with path surfaces, to alter and control a lower-limbs motion. The walking action in one step walking using the walking control method is shown in **Table 1** and **Fig. 8**. Walking motions at each phase are as follows.

I) Latter Swing Phase: The robot walks with the standard walking pattern, until the preset swing-leg landing time in the standard walking pattern, or until swing leg lands after the time.

II) Landing Phase: In this study, we define the landing phase as the period between the time when the swing leg touches the path surface or the preset landing time of the foot plate has passed on the standard walking pattern and the beginning of a double support phase on the standard walking pattern. During this phase foot lowering operation is performed using expression (2) so that the actual distance between the foot plates follow the changes in the theoretical distance between the foot plates when walking on the horizontal, smooth path on the standard walking pattern. **Fig. 9** shows the appearance of the correction of the lower-limb trajectories.

$$
\begin{aligned}
Z_{o'(n)} &= Z_{o'(n-1)} + (H_{i(n)} \cos\alpha_n - H_{r(n-1)} \cos\alpha_{n-1}) \\
X_{o'(n)} &= X_{o'(n-1)} + (H_{i(n)} \sin\alpha_n - H_{r(n-1)} \sin\alpha_{n-1})
\end{aligned}
\qquad (2)
$$

$Z_{o'(n)}, X_{o'(n)}$: The Z^m and the X^m coordinates of the origins of the detection coordinates, in the detection of landing surfaces at "n" times.

$H_{i(n)}$: The simulated distance between foot plates when walking on horizontal and flat surfaces with the standard walking patterns, in the detection of landing surfaces at "n" times.

$H_{r(n)}$: The actual distance between foot plates, in the detection of landing surfaces at "n" times.

α_n: The target angle of the upper-foot plate, in the detection of landing surfaces at "n" times.

Here, explanatory to say about the method for deciding the target angle α of the upper-foot plate, actually there are deviations in also actual models caused by the deviation of structural materials, the response delay of actuators, and the slight fluctuation of the throughout model in walking, and so on, in addition to the deviation in the shape of path surfaces. Therefore, when setting a gradient of the landing surface as a target value, the robot can not land smoothly. When setting an angle between foot plates A' *as* a target value for smooth landing, the deviation to the deviation of path surfaces becomes larger in using as

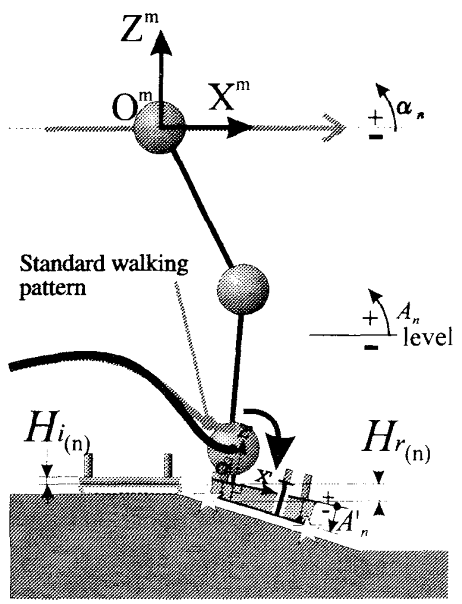

Fig. 9 Control of landing motion

supporting legs, though it can land smoothly. The target angle is decided with the expression **(3)** given below, consequently.
The weighting factors "*a*" and "*b*" were decided as 0.7 and 0.3 respectively, from the result of the walking experiment with the machine model WL-12RVII.

$$\alpha_n = a(A'_n + \alpha_{n-1}) + bA_n, a = 0.7, b = 0.3. \quad (3)$$

III) Support phase: **(III-a)** At the double support phase, the alteration and control of lower-limb trajectories with the information on landing surfaces are stopped and the lower-limb trajectories is generated in real time by the installing computer with the setting of total altering amounts as the deviation of landing surfaces, and the robot is program-controlled by this trajectory. **(III-b)** At the former single support phase, such returning control is done as returning the relative position relation of ankles and waists accepted the trajectory alteration to the relative position relation in the standard walking pattern. The alteration of trajectories in the returning control is done by the method including an interpolation with the fifth polynomial shown in the expression **(4)**, to serialize the position, velocity, and acceleration toward the X and the Y axes, to lower the deviation to the preset ZMP. **(III-c)** At the latter single support phase, the trajectory complies with the standard walking pattern, except for altering an angle of ankle joints (foot plates) in accordance with the inclination of path surfaces.

$$position(t) = a_0 t^5 + a_1 t^4 + a_2 t^3 + a_3 t^2 + a_4 t^1 + a_5 t^0 \quad (4)$$

$$a_i: coefficient, i = 0,1,2,3,4,5., t: time.$$

IV) Former Swing Phase: The angle of ankle joints (foot plate) of which the return to the standard walking pattern that does not complete is returned to the standard walking pattern, by the interpolation with the fifth polynomial.

4.3 Walking simulations

Under this walking control method, we performed adaptive walking simulations to estimate the shape deviation of the path to which the machine model will adapt. We assumed that the machine model walking did not transform the walking path at all, the model is a system of particles as shown in **Fig. 7**, the structural members of the model did not bend, and there was no delay in response of the actuators. As a result, the maximum walking speed was 1.28 s/step with a 0.3 m step length, and the adaptable deviation range was from -15 to +17 mm/step in the direction of Z axis, and from -3 to +3 ° in the tilt angle.

5 Walking experiments

The authors conducted walking experiments using the proposed walking control method and the biped walking robot WL-12RVII with WAF-3. The following a summary of the experimental results.

1. Adaptive dynamic biped walking adapting to humans' living floor with unknown shape was realized. The walking speed was 1.28 s/step with a 0.3 m step length, and the adaptable deviation range was from -16 to +16 mm/step in the direction of Z axis, and from -3 to +3 ° in the tilt angle. This result is almost corresponding to the walking simulation result.
2. On a tatami mat characteristic in Japanese living environment, the surface of which sank about 2 mm when the machine model was placed on it with a single leg supporting, stable dynamic biped walking was realized as well as on the wooden floor that hardly transformed even if the machine model walked over it.
3. Obtaining information about the gradient of the walking surface throughout all phases of dynamic walking was successfully accomplished.
4. The adaptive dynamic biped walking success probability was approximately 100% (no falls after about 50 trials).

As one example of the walking experiment result on the path with the severest conditions, **Fig. 10** and **Fig. 11** show the measurement values of the gradient of the landing path surface and the distance between upper-foot plate and lower-foot plate when WL-12RVII with WAF-3 adapted to an unknown trapezoid placed on the horizontal, smooth floor while walking eight steps including the beginning and the end of the walk. Considering human's living environment, for the walking surface, the wooden floor covered with a short-piled wool carpet is used. This walking surface sinks about 1.5 mm in the vertical direction to the surface when the machine model is supported with a single leg.

6 Conclusions

The purpose of this study is to aim at stable and practicable dynamic walking under human's living environment by a life-size robot and to achieve stable biped walking by a life-size robot that adapts in real time to the path with deviation in its shape.

The authors first developed a foot mechanism that can measure the relative position and gradient during dynamic walking.

Next, we proposed an adaptive walking control method with closed loop control system, which adapts in real time to the path with

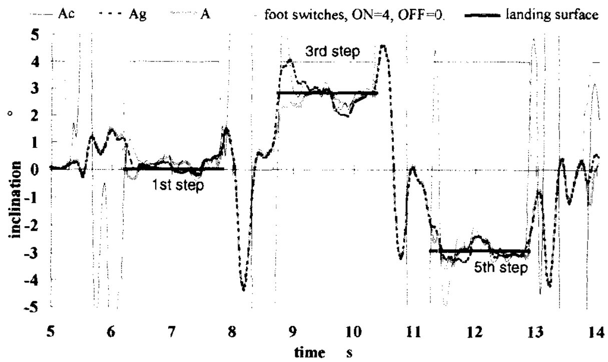

Fig. 10 Measurement results of landing surface's absolute inclination during dynamic walking adapting to an unknown trapezoidal surface. Inclination +3° (3rd step), -3° (5th step), length: 0.3 m/step, step time: 1.28 s/step, right leg.

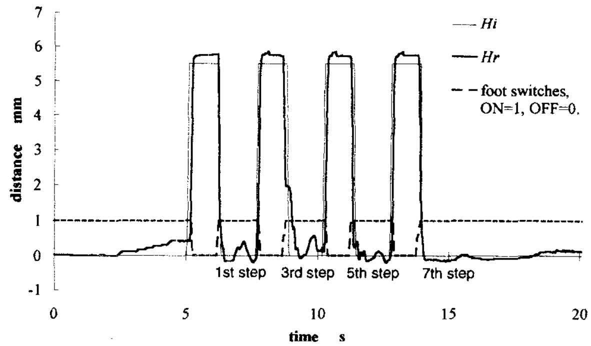

Fig. 11 Distance between upper-foot plate and lower-foot plate during dynamic walking adapting to an unknown trapezoidal surface. Inclination +3° (3rd step), -3° (5th step), length: 0.3 m/step, step time: 1.28 s/step, right leg.

deviation in its shape by using multiple pieces of information acquired from the foot mechanism developed.

In addition, performing the walking experiment using the biped walking robot developed, we achieved dynamic walking that adapts in real time to the environment with deviation in the shape of the path surface.

In conclusion, the effectiveness of the walking control method proposed in this paper and the developed walking system have been experimentally supported.

Acknowledgments

This study has been conducted as a part of the project: Humanoid at HUREL (HUmanoid REsearch Laboratory), Advanced Research Center for Science and Engineering, Waseda University. The authors would like to thank ATR, NAMCO Ltd., and YASKAWA ELECTRIC Corp., for their cooperation in this study. The authors would also like to thank ANALOG DEVICES Inc., Japan Aviation Electronics Industry, Ltd., Kuroda Precision Industries, Ltd., MOOG JAPAN Ltd., Toray Industries, Inc., and YUKEN KOGYO Co., Ltd. for supporting us in developing the hardware for a biped walking robot in the process of this study.

On June 19, 1994, The authors were deprived of a joint researcher Ichiro Kato who was Professor at Waseda University. The authors would like to thank him for his advice to this study, and pray his soul may rest in peace.

References

[1] A. Sano, J. Furusho, "Realization of natural dynamic walking using the angular momentum information", *Proceedings of the 1990 IEEE International Conference on Robotics and Automation*, pp. 1476-1481, 1990.

[2] A. Sano, J. Furusho, "Control of torque distribution for the BLR-G2 biped robot", *Proceedings of the 1991 IEEE International Conference on Robotics and Automation*, pp. 729-734, 1991.

[3] S. Kajita, T. Yamaura, A. Kobayashi, "Dynamic walking control of a biped robot along a potential energy conserving orbit", *IEEE Transaction on Robotics and Automation*, Vol. 8, No. 4, pp. 431-438, 1992.

[4] S. Kajita, K. Tani, "Study of dynamic biped locomotion on rugged terrain -theory and basic experiment-", *Proceedings of the 1991 International Conference on Advanced Robotics*, pp. 741-746, 1991.

[5] A. Takanishi Y. Egusa, M. Tochizawa, T. Takeya, I. Kato, "The realization of dynamic walking by the biped walking robot WL-10RD", *Proceedings of the 1985 International Conference on Advanced Robotics*, pp. 459-466, 1985.

[6] A. Takanishi Y. Egusa, M. Tochizawa, T. Takeya, I. Kato, "Realization of dynamic biped walking stabilized with trunk motion", *RoManSy 7: Proceedings of 7th CISM-IFToMM Symposium on Theory and Practice of Robots and Manipulators, Hermes, Paris*, pp. 68-79, 1988.

[7] A. Takanishi H. Lim, O. Tsuda, I. Kato, "Realization of dynamic biped walking stabilized by trunk motion on a sagittally uneven surface", *Proceedings of the 1990 IEEE International Workshop on Intelligent Robots and Systems*, pp. 323-330, 1990.

[8] Y. F. Zheng, J. Shen, "Gait synthesis for the SD-2 biped robot to climb sloping surface", *IEEE Transaction on Robotics and Automation*, Vol. 6, No. 1, pp. 92-102, 1990.

[9] J. Yamaguchi, A. Takanishi, and I. Kato, "Development of a Biped Walking Robot Compensating for Three-Axis Moment by Trunk Motion", *Proceedings of the 1993 IEEE/RSJ International Conference on Intelligent Robots and Systems*, pp. 561-566, 1993.

[10] J. Yamaguchi, A. Takanishi, and I. Kato, "Development of a Biped Walking Robot Adapting to a Horizontally Uneven Surface", *Proceedings of the 1994 IEEE/RSJ/GI International Conference on Intelligent Robots and Systems*, pp. 1156-1163, 1994.

[11] J. Yamaguchi, A. Takanishi, and I. Kato: "Experimental Development of Foot Mechanism with Shock Absorbing Material for Acquisition of Landing Surface Position Information and Stabilization of Dynamic Biped Walking", *Proceedings of the 1995 IEEE International Conference on Robotics and Automation*, pp. 2892-2899, 1995.